Missouri University of Science and Technology
Scholars' Mine

Chemical and Biochemical Engineering Faculty Research & Creative Works

Chemical and Biochemical Engineering

01 Jan 2005

Wetting Kinetics of Films Containing Non-Adsorbing Polymers

S. Saritha

Xianzhong Zhang

Partho Neogi
Missouri University of Science and Technology, neogi@mst.edu

Follow this and additional works at: https://scholarsmine.mst.edu/che_bioeng_facwork

 Part of the Chemical Engineering Commons

Recommended Citation

S. Saritha et al., "Wetting Kinetics of Films Containing Non-Adsorbing Polymers," *Journal of Chemical Physics*, American Institute of Physics (AIP), Jan 2005.
The definitive version is available at https://doi.org/10.1063/1.1943427

This Article - Journal is brought to you for free and open access by Scholars' Mine. It has been accepted for inclusion in Chemical and Biochemical Engineering Faculty Research & Creative Works by an authorized administrator of Scholars' Mine. This work is protected by U. S. Copyright Law. Unauthorized use including reproduction for redistribution requires the permission of the copyright holder. For more information, please contact scholarsmine@mst.edu.

HTML ABSTRACT + LINKS

Wetting kinetics of films containing nonadsorbing polymers

S. Saritha, Xianzhong Zhang, and P. Neogi[a)]
Chemical and Biological Engineering, University of Missouri-Rolla, Rolla, Missouri 65409-1230

(Received 15 February 2005; accepted 21 April 2005; published online 29 June 2005)

Kinetics of wetting by a polymer solution have been studied theoretically for a film pinned to a slot. The fluid mechanical equations have been solved using a numerical scheme. The role of polymers appears in the disjoining pressure in the model. The spreading kinetics are observed to follow a power law: a power of $\frac{1}{4}$ is observed at short times due to the Laplace pressure, and $\frac{1}{2}$ at large times under the Hamaker part of the disjoining pressure at very large times and with no equilibration. It is argued and demonstrated that techniques which have low resolutions such as microscopy will measure quite different kinetics: at short times a power of $\frac{1}{4}$ as for wetting liquids and then a sudden equilibration as reported in these experiments. It is also argued on the basis of steric exclusion, and quantified in the disjoining pressure, that the behavior returns to that of wetting liquids when the polymer molecular weight becomes very high, as also observed in the experiments. Examples of how these features can find practical applications, and hence, the importance of use of polymers as additives are given. © *2005 American Institute of Physics*. [DOI: 10.1063/1.1943427]

INTRODUCTION

The knowledge of spreading kinetics finds many applications[1] and, as a result, a considerable amount of work has been reported. One instance where an ultrathin coat of polymer is applied on a solid surface during the fabrication of microelectronic devices is considered here. The easiest way to perform this is to layer a thin film of polymer solution on the solid surface and then evaporate the solvent. However, Klein and co-workers[2–6] found that such films were nonwetting and broke up into beads. Since the substrates used, such as glass slides, silicon wafers, etc., have high surface energies, low-surface-energy polymer solutions should have wetted the surfaces.[7] Nieh *et al.*[8] have reported the values of equilibrium contact angles as functions of polymer concentration and molecular weight. In all the above cases, the polymers were judged to be nonadsorbing. Ybarra *et al.*[9] have explained the equilibrium results using the properties of thin liquid films. A simple view of the shape of the contact line for a nonwetting liquid at equilibrium is shown in Fig. 1(a) in the form of a wedge. For a wetting liquid, there is no equilibrium and the liquid spreads out until a thin film of constant thickness is reached everywhere. There is yet one other kind of equilibrium configuration. Derjaguin[10] and Frumkin[11] have shown that if the added potential in thin films in the form of disjoining pressure is considered, then a wedge can form in equilibrium with a thin film of constant thickness. However, the disjoining pressure must have a part that promotes thinning (such as London–van der Waals forces) and a part that prevents thinning, which the nonadsorbing polymers do. In that case the wedge angle λ is the contact angle and one has

$$\cos\lambda = 1 + \frac{1}{\gamma}\int_{h_0}^{\infty} \Pi(h)dh, \tag{1}$$

where Π is the disjoining pressure and γ is the surface tension. As shown in Fig. 1(a), the wedge does not taper to a point, but forms a thin film of constant thickness h_0. In this film, the two opposing forces mentioned earlier balance one another and $\Pi(h_0)=0$ for a wedge. The thickness h_0 is much larger than the molecular dimensions, but cannot be observed under a microscope. Ybarra *et al.*[9] have used the excess energy of nonadsorbing thin films calculated by Daoud and de Gennes[12] to obtain

$$\Pi = \frac{A_H}{12\pi h^3} - \frac{RT\phi_\infty \rho_p}{M} N\left(\frac{b}{h}\right)^{5/3}, \tag{2}$$

where the first term on the right represents the Hamaker interaction. The volume fraction of the polymer in the main drop is ϕ_∞, the density of the polymer is ρ_p, N is the number of steps in the polymer, b is the step size, and M is the molecular weight of the monomer. The second term is due to the polymer and arises when the effect of change in the conformation of the polymer as it is squeezed into the thin film is considered. Use of Eqs. (1) and (2) and the appropriate equilibrium relations led them to calculate the contact angle λ. These values were found to be small in keeping with the experimental results. In addition, on increasing the molecular weights of the polymer ($\sim 10^6$) it was found that the system returned to wetting, as seen in the experiments.[8]

The characteristics of wetting kinetics which determine the efficacy of the accompanying coating process are of importance. The observations on the kinetics of spreading made by Nieh *et al.*[8] are peculiar. They reported that the drops spread with the rate expected of wetting liquids. If r_0 is the basal radius, then $r_0 \propto t^{1/10}$ for wetting liquids. However, the spreading drops stopped almost suddenly to equilibrate. This behavior has been noted by Zosel[13] as well. Nieh *et al.*[8] also

a)Electronic mail: neogi@umr.edu

 © 2005 American Institute of Physics

Downloaded 12 May 2008 to 131.151.26.225. Redistribution subject to AIP license or copyright; see http://jcp.aip.org/jcp/copyright.jsp

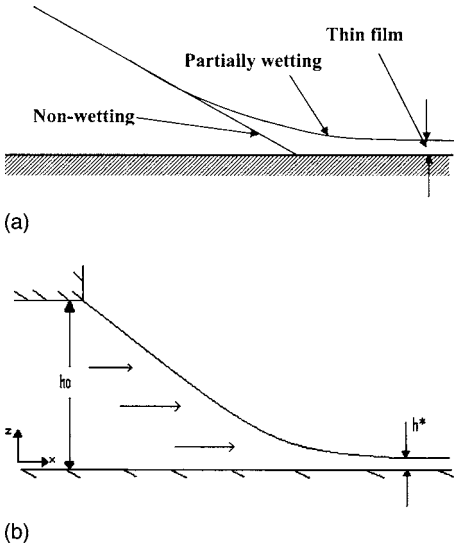

FIG. 1. (a) The profile of a nonwetting liquid near the contact line is just a wedge. The liquids described by Eq. (1) also posses a wedge and the wedge angle is the equilibrium contact angle. However, it thins down to a film of constant thickness instead of converging to a sharp point. Solutions of nonadsorbing polymers fall in this category. Only a thin film of constant thickness can be formed with wetting liquids. (b) Schematic view of the flow from the slot. The film thickness is h at any location, $h=h_0$ at the slot mouth and h^* at the contact line.

found that at high polymer concentrations (40 wt %) the more predictable behavior, that the spreading rate of the drop decreased continuously to zero at equilibrium, was seen. In view of the earlier work that explained the equilibrium behavior using thin-film phenomena, it becomes important to consider the kinetics of wetting where the disjoining pressure that is capable of equilibrating the drop is included. That is, this form of the disjoining pressure is considered below. We also have some expectations that the sudden-stop behavior and the kinetics of wetting which follows that of wetting liquids can be explained this way.

Experiments on wetting kinetics are carried out in a contact angle goniometer, which has an error of about ± 14 μm in their linear measurements. As a result small drops can be observed, but not the thin films, as shown in Fig. 1(a). In addition, if the contact line is defined where the local film thickness $h=0$, it becomes apparent that its location can only be approximated when h is of the order of 14 μm instead of zero. In contrast, the resolution in differential ellipsometry is at ± 0.1 nm.[14] The "drops" studied here are often vapor deposited. In practically all cases studied by ellipsometry, the macroscopic thicknesses of these drops are within values where the disjoining pressure dominates. This makes the spreading kinetics different. In particular, the contact line is located at a thickness of ~ 0.1 nm. This too has an impact in that at $h=14$ μm a macrodrop will feel very different forces of spreading than at $h=0.1$ nm.

Most practical problems in wetting have macroscales much greater than the thickness over which the disjoining pressure is important. Consequently, it is necessary to analyze problems where the macroscale is at least 100 nm, the largest thickness where the effects of the disjoining pressure can be detected. Such results have been reported earlier[15] for wetting liquids containing no polymers. One feature that was reported in those calculations is that even when the speed at $h=1$ nm is taken to be the spreading velocity, the rates are seen to be dominated by the effects of surface tension, until at exceptionally large times when the rates become those determined by the disjoining pressure. Those liquids that were studied have no equilibrium, but the polymer solutions considered here do. It becomes conceivable that drops of polymer solutions at film thickness $h=14$ μm will see equilibration even at times where the spreading is determined by surface tension. This would explain why the $t^{1/10}$ rate is observed.

In the next section, the formulation and the method of solution are discussed. These have been covered in brief as they have seen more detailed discussion earlier.[15]

FORMULATION

The film is thin and flat and the lubrication theory approximation can be used. Under this approximation, the momentum equations are solved under the assumptions that the flow is mainly in the tangential direction (x) and varies only in the normal direction (z). The system of coordinates is shown in Fig. 1(b), along with some key parameters. Using the no-slip boundary condition on the solid surface and zero shear at the air–liquid interface, the velocity is averaged in the normal direction and used in the continuity equation to get an equation for the film profile[15]

$$\frac{\partial h}{\partial t} = \frac{1}{3\mu}\frac{\partial}{\partial x}\left[h^3\frac{\partial P}{\partial x}\right], \tag{3}$$

where the total pressure is the sum of the Laplace pressure and the disjoining pressure

$$P = -\gamma\frac{\partial^2 h}{\partial x^2} + \Pi(h). \tag{4}$$

In addition, a term in the disjoining pressure is introduced,

$$\Pi = \frac{A_H}{12\pi h^3} - \frac{RT\phi_\infty\rho_p}{M}N\left(\frac{b}{h}\right)^{5/3}e^{-N(b/h)^{5/3}}, \tag{5}$$

where $\phi_\infty e^{-N(b/h)^{5/3}}$ is the local polymer volume fraction ϕ, which is different from the reservoir value ϕ_∞. This difference occurs because it is difficult to squeeze a polymer into a thin film. The exponential term is the Boltzmann factor, where the energy used is $-T\Delta S$, which also occurs in the disjoining pressure with some modifications. Here ΔS is the change of entropy of the polymer molecule. At equilibrium, thermodynamic calculations can be made[9] to show the exact differences between the two concentrations, but we have a dynamic system here. Consequently, the Boltzmann term is used both for its simplicity and for the fact that it follows qualitatively the right trend in excluding polymers from very thin films.

Nondimensionalizing Eqs. (3) and (4) leads to

$$\frac{\partial H}{\partial T} = \frac{1}{R^2}\frac{\partial}{\partial X}\left[\frac{H^3}{3}\frac{\partial \wp}{\partial X}\right], \tag{6}$$

Downloaded 12 May 2008 to 131.151.26.225. Redistribution subject to AIP license or copyright; see http://jcp.aip.org/jcp/copyright.jsp

$$\wp = -\frac{1}{R^2}\frac{\partial^2 H}{\partial X^2} + \bar{\Pi}, \tag{7}$$

where $H=h/h_0$, $X=x/x_0$, $R=x_0/x_0(0)$ $\bar{\Pi}=(h_0{}^2/\gamma x_0(0))\Pi$, $T=(\gamma/\mu x_0(0))t$, and $\wp=(h_0{}^2/\gamma x_0(0))P$. Here x_0 determines the position of the contact line, $x_0(0)$ is the initial position of the contact line, and h_0 is the thickness of the film at $x=0$.

With no forced spreading, the Laplace pressure is zero at the mouth of the slit ($X=0$). Also, the slope at the contact line ($X=1$) is zero. The other boundary conditions used in solving the above equations are H equal to 1 at the slit mouth and H^* at the contact line, where H is the dimensionless thickness equal to h/h_0 and $H^*=h^*(=1\text{ nm})/h_0$. The equations are solved using forward-time-central-space (FTCS) scheme [and not central-time-forward-space (CTFS) stated incorrectly by Zhang *et al.*[15]]. A simplified initial profile of a straight line with a steep slope was chosen. This was used to subsequently update the position of the contact line at a later time, using the equations of average velocity in the tangential direction,

$$\langle v_x\rangle|_{x=x_0} = \frac{dx_0}{dt}, \tag{8}$$

$$\langle v_x\rangle = -\frac{h^2}{3\mu}\frac{\partial P}{\partial x}. \tag{9}$$

Note that $h=h^*$ at $X=1$ in Eq. (8). Instead of evaluating the left-hand side in Eq. (8) at $X=1$, the present scheme allows us to evaluate it only at $X=0.99$. The reason for this shortcoming is discussed by Zhang *et al.*,[15] who also showed that there are no accompanying ill effects. The film thickness at this effective contact line is found to lie between $h=1-2$ nm, instead of 1 nm that would be seen at $X=1$. A small initial time step was chosen, which was gradually increased in order to speed up the computation. It should be noted that the liquid has been assumed to be a Newtonian liquid even though a polymer solution is being analyzed. This assumption has been made since Nieh *et al.*[8] have observed in their experiments that there was no distinction between the quantitative behavior of a Newtonian fluid and a shear-thinning polymer solution. Some theoretical justification is also available. Neogi and Ybarra[16] have shown theoretically, using the method of de Gennes[17] that shear-thinning liquids behave like Newtonian fluids with viscosities equal to their zero-shear viscosities.

All physical parameters have been taken from Ybarra *et al.*,[9] corresponding to polystyrene (molecular weight 45 000) dissolved in dibutyl phthalate. These are $\rho_p=0.8\ \text{g/cm}^3$, $b=5$ nm, and for the solvent $M/N=104$ =molecular weight of the solvent under the lattice theory. The effective volume fraction of the polymer in the reservoir $\phi_\infty=0.05$.

RESULTS AND DISCUSSION

Both due to the small step sizes and the complexity of the expressions in Eq. (5), it took about one year of computation time to complete the calculations on a workstation. The extent of spreading as a function of time is shown in Fig. 2. Two cases were considered, one for $h_0=100$ nm and $x_0(0)=400$ nm and one for $h_0=50$ nm and $x_0(0)=200$ nm. Both cases follow the power rule, and the slope rises from the value of $\frac{1}{4}$ to that of $\frac{1}{2}$. Zhang *et al.*[15] have shown that in the absence of polymers, the spreading rates show a sharp transition from surface-tension-driven flow (slope of $\frac{1}{4}$ power) to disjoining-pressure- (exclusively Hamaker forces) driven flow (slope of $\frac{1}{2}$ power). The dashed line of slope $\frac{1}{4}$ in Fig. 2 has been used to aid the eye. In the 50-nm case, the results for thin films with polymer are identical to those without polymer.[15] The transition between the two slopes takes place earlier than where $h_0=100$ nm because of the increased importance of the disjoining pressure when the macroscale is smaller. Where $h_0=100$ nm, it is also seen that the system containing the dissolved polymer spreads slower than without polymer. One plausible explanation is given below. If we section Figs. 3(a) and 3(b) into two horizontal strips, then the top strip will be dominated by surface-tension forces. This strip also is the thickest strip. The bottom strip is a very thin one and is dominated by London–van der Waals forces. In the case where the film is thin, $h_0=50$ nm, these two regions overlap. Where the films are thicker, $h_0=100$ nm, a middle panel is possible, where the repulsion forces due to the polymer can be felt. This would help retard the spreading. Nevertheless, the effect of polymers is sufficiently strong in both cases such that at equilibrium a thin film of constant thickness develops at the contact line.

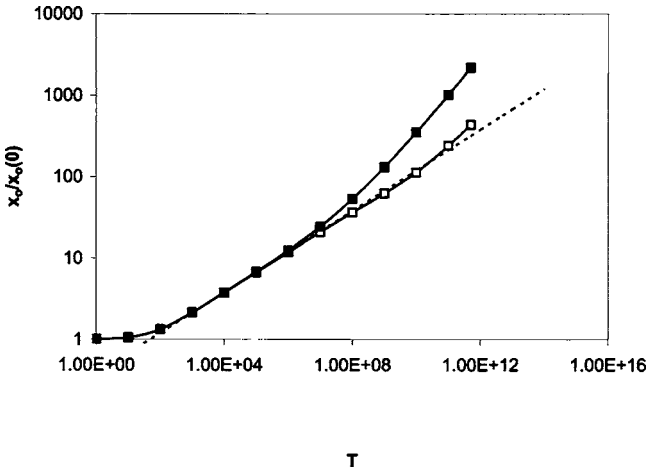

FIG. 2. The results for liquid-containing polymers have been shown for the two cases of $h_0=100$ nm (white squares) and $h_0=50$ nm (solid black squares). The dashed line represents the asymptotic $\frac{1}{4}$ slope, which is an indication of surface-tension-driven flow. At larger times the slope increases to a power of $\frac{1}{2}$, which is disjoining-pressure-driven flow determined by Hamaker forces only.

We emphasize that these results of spreading kinetics apply when the measurements are taken at $h=1-2$ nm, or in dimensionless form at $H\approx 0.01$. As stated earlier, it is possible to suggest that this would be the outcome using measuring techniques with dimensionless errors of ±0.01. Up to this point, it is seen that the effects of added polymer are not detectable, except in one case where there is a small slowing down.

The profiles provide interesting details. These have been shown at various times for the case of $h_0=100$ nm in Fig.

Downloaded 12 May 2008 to 131.151.26.225. Redistribution subject to AIP license or copyright; see http://jcp.aip.org/jcp/copyright.jsp

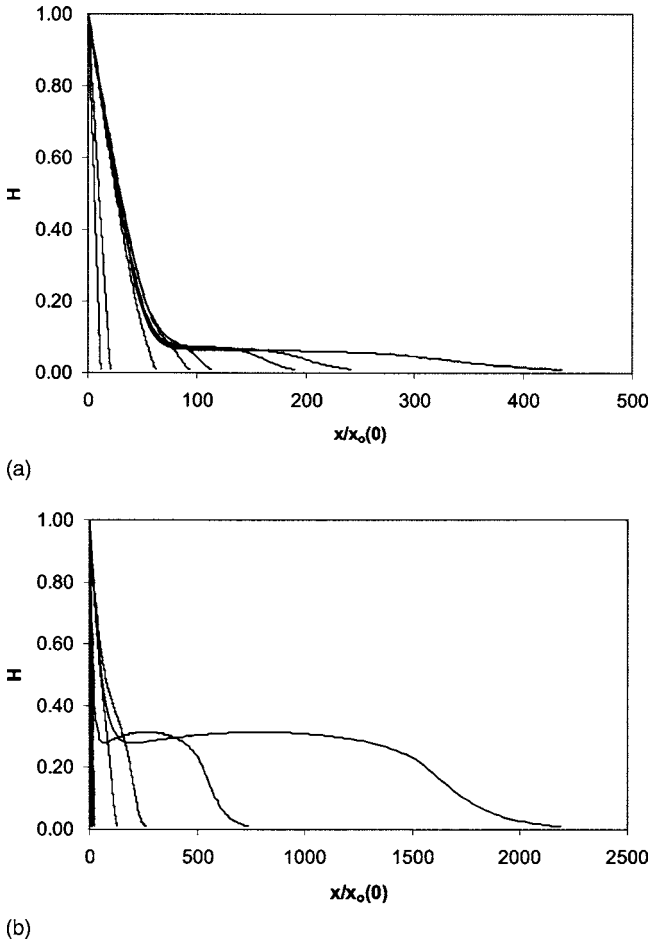

FIG. 3. (a) The film profiles have been shown in the form of dimensionless thickness vs spreading for the case when $h_0=100$ nm. There are two parts of the film profile, the macroscopic part, which reaches equilibrium much before the thin-film region, and the thin-film region, which continues to spread and does not attain equilibrium. From left to right, the plots are shown at dimensionless time $T=1\times10^6$, 1×10^7, 1×10^9, 5×10^9, 1×10^{10}, 5×10^{10}, 1×10^{11}, and 5×10^{11}. (b) The same as in Fig. 3(a) for $h_0=50$ nm. From left to right, the plots are shown at dimensionless time $T=1\times10^6$, 1×10^7, 1×10^9, 5×10^9, 5×10^{10}, and 5×10^{11}.

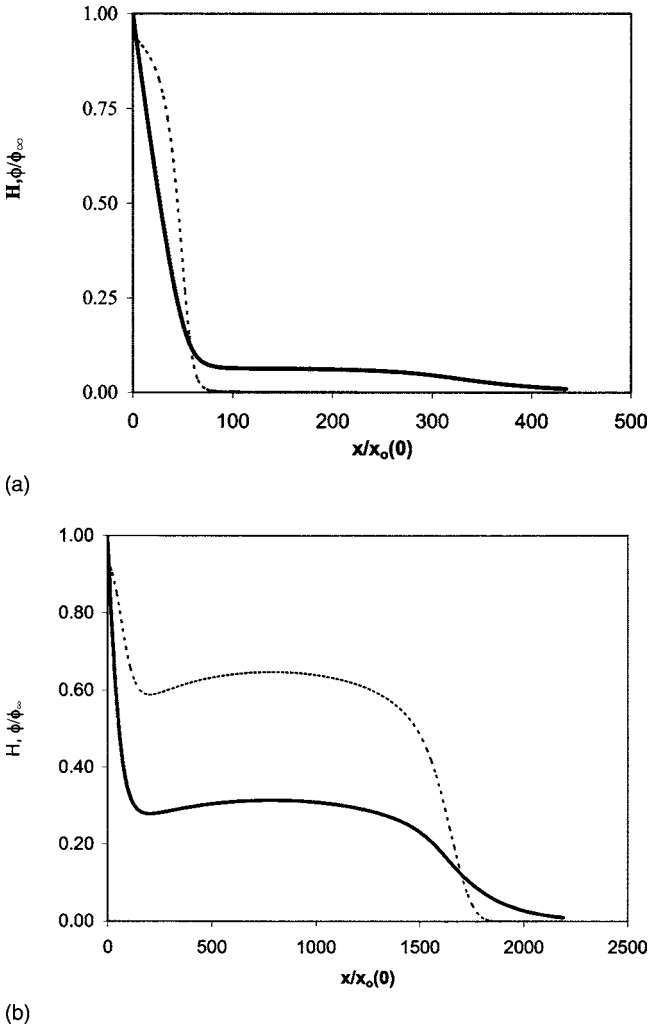

FIG. 4. (a) The film profile (bold line) at the largest time as well as the dimensionless polymer concentration $\phi/\phi_\infty=e^{-N(b/h)^{5/3}}$ and the Boltzmann factor (dashed line) have been shown at the largest time for $h_0=100$ nm. The polymer concentration in the thin-film region is nearly zero. $T=5\times10^{11}$. (b) The same as in Fig. 4(a) for $h_0=50$ nm. $T=5\times10^{11}$.

3(a) and for $h_0=50$ nm in Fig. 3(b). The macroscopic profiles reach equilibrium in the first phase and in the second phase a thin film (microscopic) is established, which does not reach equilibrium. At this point we revisit the Boltzmann factor $e^{-N(b/h)^{5/3}}$, which shows the polymer concentration to be nearly zero in the thin film. These are shown in Figs. 4(a) and 4(b) for the two cases of $h_0=100$ nm and $h_0=50$ nm. Note that in the second case, considerable penetration of the polymer into the thin film has occurred. Nevertheless, the polymer concentration drops to zero by the time the contact line is approached. Both Figs. 4(a) and 4(b) are at $T=5\times10^{11}$. It clearly shows why the movement of the contact line discussed in the above section is dominated by Hamaker forces at large times. It is obvious that the thin film will not be seen if the magnification is not high. Using arguments given earlier, if the measuring technique has the larger dimensionless error of ±0.5, then the contact line would be measured at the dimensionless thickness of $H\approx0.5$. This new contact line speed is bound to show equilibrium, as seen in Fig. 5. Of importance is the fact that before equilibration, both plots (corresponding to high and low magnifications) show the same slope of $\frac{1}{4}$. This is the region of surface-tension-driven flow. The profiles in Fig. 3 show that up to equilibration in the thick film, no thin-film region is established. Thus, all of the flow is indeed determined by the surface-tension forces up to that point. These results also compare favorably to the experimental observations on drops where Nieh *et al.*[8] report that drops of polymer solution spread with time, showing a power of 1/10 which is indicative of surface-tension-driven flows. Using microscopy, they also observed a sudden stop. In Fig. 5 it is seen that the extent of spread determined at low resolution decreases a little upon equilibration. This small dip is not possible to verify experimentally since it is possible to wait twice the equilibration times in the experiments, but not over two orders of magnitude as indicated in the figure.

One key feature that emerges from this study is that it does not mean that the liquid is wetting when the spreading is found to be driven by surface tension ($\propto t^{1/4}$). The only way to confirm this is to wait for sufficiently large times.

To help classify clearly the different cases, the behavior

Downloaded 12 May 2008 to 131.151.26.225. Redistribution subject to AIP license or copyright; see http://jcp.aip.org/jcp/copyright.jsp

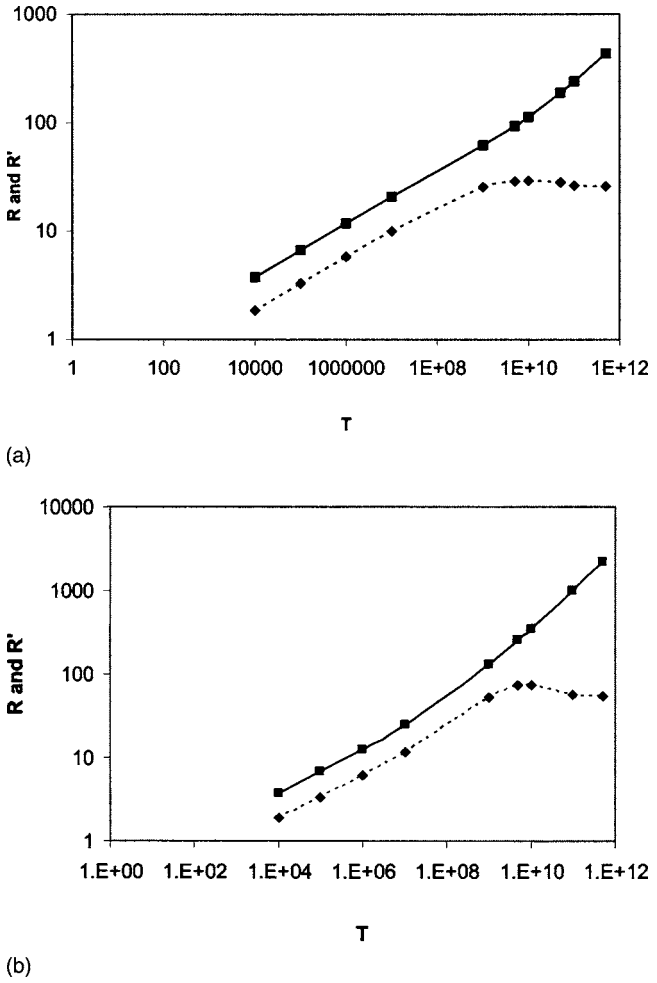

FIG. 5. (a) The contact line measured with two different dimensionless resolutions has been shown for $h_0=100$ nm. The lower line which attains equilibrium is for a dimensionless resolution of ± 0.5 (R' dashed line), while the upper line which continues to rise is for a resolution of ± 0.01 (R bold line). (b) The same as in Fig. 5(a) for $h_0=50$ nm.

in a system containing a well-defined contact line [see Fig. 1(a)] is described in brief. This case has been studied theoretically by Neogi and Miller[18] and shows only a gradual move towards equilibrium. If the macroscopic wedge angle is defined as the dynamic contact angle α (and one that will be measured using low-resolution methods such as microscopy commonly in use), then at short times $\alpha \gg \lambda$, the equilibrium angle. For such times, the drop does move at the same rate as that for a wetting liquid. The manner in which equilibrium is reached, as observed under microscopy, is, however, *gradual* in contrast to the case studied here, which is characterized by sudden equilibration. This gradual equilibration is also observed in polymer solutions, but at large polymer concentrations,[8] and remains as the only case that we cannot predict because the disjoining pressure used does not apply at large concentrations.

Some results of practical importance are now determined. Where the thin liquid films are not of interest, we are able to compress their effects into boundary conditions for solving problems of interest at the macroscale. Thus, (a) where there is partial wetting at equilibrium and (b) where observations are being made at resolutions no better than in microscopy,

$$\frac{dx_0}{dt} = \frac{\gamma}{6\mu}\left[\ln\left|\frac{1}{\varepsilon}\right|\right]^{-1}\alpha^3 \quad \alpha > \lambda, \tag{10a}$$

$$=0 \quad \alpha = \lambda, \tag{10b}$$

$$=-\frac{\gamma}{6\mu}\left[\ln\left|\frac{1}{\varepsilon}\right|\right]^{-1}\alpha(\lambda^2-\alpha^2) \quad \alpha < \lambda. \tag{10c}$$

Here ε is the ratio of slip length to the macroscopic length scale and is equivalent to h^*/h_0 here. Now, Eq. (10a) is the full form of wetting kinetics for a wetting liquid as obtained by de Gennes.[17] Equations (10a) and (10b) describe the sudden stop. Equation (10c) is from Brochard–Wyart and de Gennes,[19] modified by the results of Neogi and Miller[18] (see Neogi[20] for further discussion), and describes a receding contact line with an equilibrium contact angle λ defined by Eq. (1). It has been conjectured above that in the case of an overshoot, the system will return to equilibrium.

We return to the process of layering of ultrathin polymer films on substrates starting with thin films of polymer solution. Consider the Boltzmann factor $e^{-N(b/h)^{5/3}}$ when the molecular weight of the polymer is high $\sim 10^6$. For the parameters used here, the exponential term is negligible up to $h=150$ nm. That means the fluid which emerges from the slot is free of polymer and is wetting as the solvent is wetting. Of course, we know that the Boltzmann factor is a simple approximation, but it shows that the larger the molecular weight of the polymer, the larger is the film thickness over which the filtering effect is observed. In Figs. 1 and 3, the contact line can be taken to be at the junction between the bulk and the thin film. The above result implies that as the molecular weight is increased, this contact line will not get pinned, that is, it will not reach equilibrium. This has been verified experimentally by Nieh *et al.*[8] In that, we provide a better alternative to spreading a thin layer of polymer solution by using a polymer of large molecular weight than Klein and co-workers who suggest difficult substrate modifications. Our method can also be used in conventional coating processes.

In summary, we find that the thin-film phenomena are able to explain the main observations in the experiments as well as provide a practical guide as to how to manipulate wettability and wetting kinetics using polymers as additives. We fall short of predicting the observations at large polymer concentrations since Eq. (2) is not valid there.

ACKNOWLEDGMENT

This material is based on the work supported by the National Science Foundation under Grant No. CTS-0228834.

[1] P. Neogi and C. A. Miller, in *Thin Liquid Film Phenomena*, AICHE Symposium Series, edited by W. B. Krantz, D. T. Wasan, and R. K. Jain (AICHE, New York, 1986), p. 145.
[2] R. Yerushalmi-Rozen and J. Klein, Prog. Rubber Plastics Ind. **12**, 30 (1996).
[3] R. Yerushalmi-Rozen and J. Klein, Langmuir **11**, 2806 (1995).
[4] R. Yerushalmi-Rozen and J. Klein, Science **263**, 793 (1994).
[5] R. Yerushalmi-Rozen and J. Klein, Phys. World **8**, 30 (1995).
[6] T. Kerle, R. Yerushalmi-Rozen, and J. Klein, Macromolecules **31**, 422 (1998).
[7] W. A. Zisman, *Contact Angle Wettability and Adhesion*, Advances in

Downloaded 12 May 2008 to 131.151.26.225. Redistribution subject to AIP license or copyright; see http://jcp.aip.org/jcp/copyright.jsp

Chemistry Series Vol. 43 (American Chemical, Society, Washington, DC, 1964), p. 1.
[8] S.-Y. Nieh, R. M. Ybarra, and P. Neogi, Macromolecules **29**, 320 (1996).
[9] R. M. Ybarra, P. Neogi, and J. M. D. MacElroy, Ind. Eng. Chem. Res. **37**, 427 (1998).
[10] B. V. Derjaguin, Zh. Fiz. Khim. **14**, 37 (1940).
[11] A. Frumkin, Zh. Fiz. Khim. **12**, 137 (1940).
[12] M. Daoud and P. G. de Gennes, J. Phys. (Paris) **38**, 85 (1977).
[13] A. Zosel, Colloid Polym. Sci. **271**, 680 (1993).
[14] A. M. Cazabat, Adv. Colloid Interface Sci. **42**, 65 (1992).
[15] X. Zhang, S. Saritha, and P. Neogi, Ind. Eng. Chem. Res. **44**, 1204 (2005).
[16] P. Neogi and R. M. Ybarra, J. Chem. Phys. **115**, 7811 (2001).
[17] P. G. de Gennes, C. R. Acad. Sci., Ser. II: Mec., Phys., Chim., Sci. Terre Univers **298**, 111 (1984).
[18] P. Neogi and C. A. Miller, J. Colloid Interface Sci. **86**, 525 (1982).
[19] F. Brochard-Wyart and P. G. de Gennes, Adv. Colloid Interface Sci. **39**, 1 (1992).
[20] P. Neogi, J. Chem. Phys. **115**, 3342 (2001).

Downloaded 12 May 2008 to 131.151.26.225. Redistribution subject to AIP license or copyright; see http://jcp.aip.org/jcp/copyright.jsp